THE GEOLOGICAL SOCIETY OF AMERICA®

Timing and mechanism of the rise of the Shillong Plateau in the Himalayan foreland

G. Govin[1†], Y. Najman[1], A. Copley[2], I. Millar[3], P. van der Beek[4], P. Huyghe[4], D. Grujic[5], and J. Davenport[6]
[1]Lancaster Environment Centre, Lancaster University, Lancaster LA1 4YQ, UK
[2]Department of Earth Sciences, Cambridge University, Cambridge CB2 3EQ, UK
[3]NERC Isotope Geosciences Laboratory, British Geological Survey, Keyworth, Nottingham NG12 5GG, UK
[4]ISTerre, Université Grenoble Alpes, 38058 Grenoble Cedex 9, France
[5]Department of Earth Sciences, Dalhousie University, Halifax B3H 4R2, Canada
[6]Centre de Recherches Pétrographiques et Géochimiques (CRPG), 54500 Vandœuvre-Lès-Nancy, France

ABSTRACT

The Shillong Plateau (northeastern India) constitutes the only significant topography in the Himalayan foreland. Knowledge of its surface uplift history is key to understanding topographic development and unraveling tectonic–climate–topographic coupling in the eastern Himalaya. We use the sedimentary record of the Himalayan foreland basin north of the Shillong Plateau to show that the paleo-Brahmaputra river was redirected north and west by the rising plateau at 5.2–4.9 Ma. We suggest that onset of plateau uplift is a result of increased fault-slip rates in response to stresses caused by the Indian lithosphere bending beneath the Himalaya.

INTRODUCTION

Unraveling the topographic evolution of mountain ranges remains a challenge. We address this question in the Shillong Plateau (SP), a 1600-m-high fault-bounded basement uplift in the Himalayan foreland (northeastern India; Fig. 1), the uplift history of which is linked to both orographic rainfall patterns and strain partitioning in the eastern Himalaya (Clark and Bilham, 2008; Coutand et al., 2014; Grujic et al., 2006).

Low-temperature thermochronology data indicate that exhumation of the SP initiated between ca. 9 and 15 Ma (Biswas et al., 2007; Clark and Bilham, 2008), whereas surface uplift of sufficient magnitude to create local flexural loading of the Indian plate is only observed by ca. 2–3.5 Ma (Najman et al., 2016). Surface uplift is therefore decoupled from exhumation for much of the plateau's history, and occurred after a period when rock uplift was compensated by surface erosion (Biswas et al., 2007). The causes and timing of the initiation of surface uplift remain uncertain.

Here, we establish the first direct estimate for the timing of onset of surface uplift, deduce a causal mechanism, and examine the relative roles of tectonics and erosion in the temporal evolution of topography in the SP. Our work advances the discussion regarding the relative importance of strain partitioning (Clark and Bilham, 2008; Coutand et al., 2014) versus orographic precipitation linked to SP uplift (Grujic et al., 2006) in influencing Himalayan exhumation rates to its north, and provides a framework for interpreting the present-day crustal structure of the SP and flanking regions (e.g., Mitra et al., 2005; Singh et al., 2016). Additionally, we provide new insights into the behavior of basement-cored foreland uplifts applicable to other orogens (e.g., Jordan and Allmendinger, 1986; Kober et al., 2013), as well as to older ranges where early records of uplift have been destroyed.

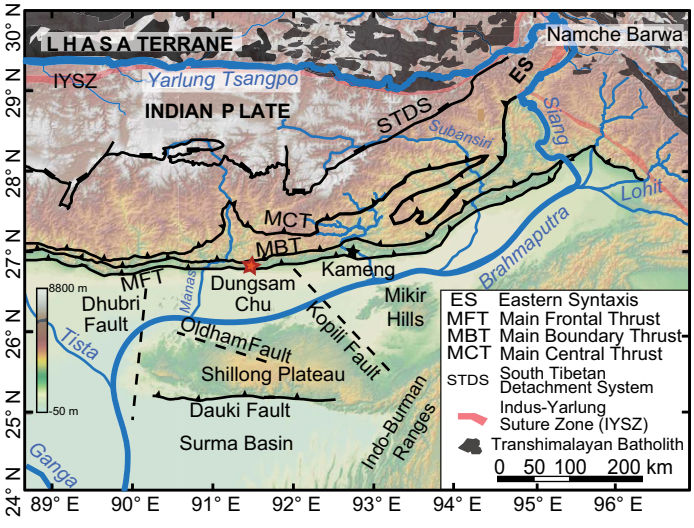

Figure 1. Main geologic features of the eastern Himalaya (from Lang and Huntington, 2014; Long et al., 2011). Red and black stars represent the Dungsam Chu (DC) and Kameng sections, respectively.

GEOLOGICAL CONTEXT AND APPROACH

The SP and adjacent Mikir Hills expose Proterozoic-Paleozoic basement overlain by outliers of Cenozoic sedimentary rocks (Mitra and Mitra, 2001). The plateau is bounded by two active crustal-scale reverse faults (Mitra et al., 2005): the Oldham and Dauki faults (Fig. 1). The latter juxtaposes basement against the Cenozoic sediments of the Surma Basin to the south, with a vertical offset of ~10 km (Biswas et al., 2007). The SP has been uplifted either as a symmetric pop-up (England and Bilham, 2015), along the Dauki fault acting as a north-dipping thrust connected to the Himalayan orogen (Seeber and Armbruster, 1981), as a crustal-scale fault-propagation fold (Clark and Bilham, 2008), or as an asymmetric basement-cored uplift (Biswas et al., 2007). Surface uplift of the SP, along with westward propagation of the Indo-Burman Ranges (IBR) (Fig. 1), diverted the Brahmaputra River northward from a south-southwest course, to flow between the Himalaya and the SP (Chirouze et al., 2013; Johnson and Alam, 1991; Najman et al., 2016; Uddin and Lundberg, 1999). Therefore, the first occurrence of paleo-Brahmaputra deposits in the basin directly north of the SP allows the initiation of surface uplift to be dated. Because only limited topographic uplift is required before river diversion occurs, this approach dates initiation of SP uplift more sensitively than flexural modeling (Najman et al., 2016), for which a significant load must be established.

Brahmaputra deposits are readily identified in the sedimentary record because the river's upstream continuation, the Yarlung River, drains the Indus-Yarlung suture zone and Transhimalayan batholiths of the Asian

†Deceased

Lhasa terrane. In contrast, Himalayan rivers only drain Indian plate rocks to the south (Bracciali et al., 2015; Cina et al., 2009; Gehrels et al., 2011). Transhimalayan detritus in dated Siwalik sediments of the eastern Himalaya shows that the Yarlung and Brahmaputra were connected by 13 Ma; connection through the Siang River (Fig. 1) was established by at least 7 Ma (Bracciali et al., 2016; Chirouze et al., 2013; Cina et al., 2009; Govin, 2017; Lang and Huntington, 2014; Lang et al., 2016).

Using new and published provenance analyses from Himalayan foreland-basin rocks, we reconstruct Brahmaputra drainage from Late Miocene to present, and determine when the river was deflected due to the initiation of uplift of the SP. By combining this work with a model for the regional stress field, we assess the cause of the transition from exhumation to surface uplift.

RESULTS: PROVENANCE ANALYSIS

We report detrital zircon U-Pb data from the Dungsam Chu (DC) section in Bhutan, located directly north of the SP (Figs. 1 and 2). We can identify paleo-Brahmaputra input to the sediments because Transhimalayan zircons are typically of Cretaceous–Eocene age. In contrast, zircons derived from Indian-plate Himalayan drainages are dominated by >400 Ma and Miocene ages (e.g., Bracciali et al., 2016; Cina et al., 2009; Gehrels et al., 2011; Lang and Huntington, 2014; Fig. 2).

Zircons from eight sandstones from the DC section (see the GSA Data Repository[1]), magnetostratigraphically dated between 7 and 1 Ma (Coutand et al., 2016), were U-Pb dated using ion-microprobe and inductively coupled plasma–mass spectrometry (ICPMS) techniques (see Data Repository sections 2–6). Samples ≤4.9 Ma show 13%–22% Cretaceous–Cenozoic grains, which we interpret as being derived from the Transhimalaya (Fig. 2). In contrast, samples ≥5.2 Ma do not contain grains of such age (Fig. 2). These data therefore show a shift to Brahmaputra-type values at 5.2–4.9 Ma. Rutile U-Pb dating of sample SJ8 (depositional age 4.9 Ma) returned 25 out of 92 ages unique to the syntaxis (U-Pb ages <9 Ma; Bracciali et al., 2016; Data Repository sections 2 and 7), also demonstrating that these deposits are sourced from the Siang River.

DISCUSSION

Brahmaputra Paleo-Drainage

We combine our new sediment provenance results with existing studies from northeast, northwest, and south of the SP to form an evolutionary model of Brahmaputra drainage (Fig. 3). Our combined zircon and rutile U-Pb age-dating provides an unambiguous signature of the paleo-Brahmaputra draining through the Siang and axially along the foreland, rather than a hypothetical transverse drainage (Cina et al., 2009). Moreover, documentation of Transhimalayan-derived detritus upstream (east) of the location of the hypothesized transverse drainage (Govin, 2017; Lang and Huntington, 2014) invalidates the Cina et al. (2009) model. Therefore, the arrival of Transhimalayan detritus at DC at 5.2–4.9 Ma reflects northwest diversion of the paleo-Brahmaputra River to this locality. Prior to this time, DC sediments were sourced exclusively by rivers draining the southern Himalaya. Because of its location relative to the SP, encroachment of the Brahmaputra to the DC section likely occurred due to uplift of the SP. The timing of uplift is consistent with a recent estimate based on incision rates in the SP (Rosenkranz et al., 2018).

Prior to 7 Ma, the Brahmaputra flowed directly south-southwest to the Bengal Fan (Fig. 3A; Uddin and Lundberg, 1999). By 7 Ma, provenance

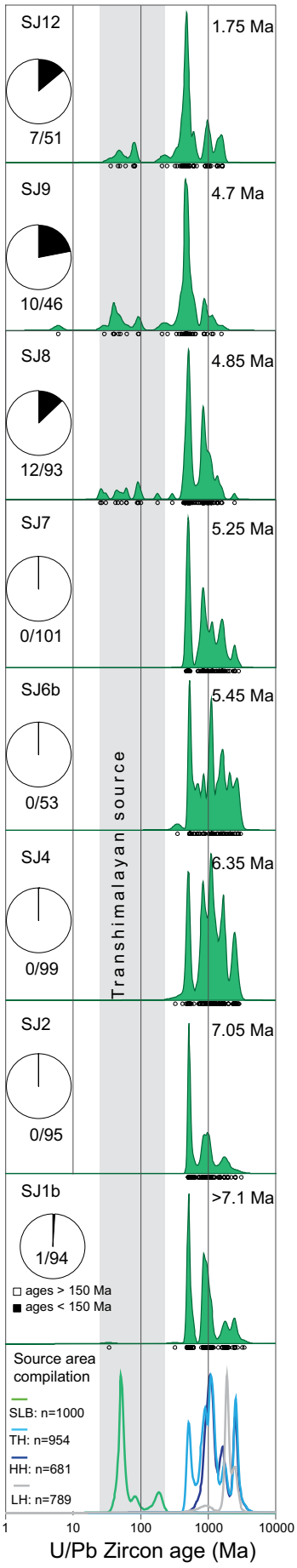

Figure 2. Kernel density plots (Vermeesch, 2012) of detrital zircon U-Pb ages from the Dungsam Chu (DC) section in the Himalaya. Depositional ages (numbers in top right) are from Coutand et al. (2016), location information is provided in the Data Repository (see footnote 1). Source area compilation is from Hu et al. (2012, and references therein). SLB—South Lhasa Block, TH, HH and LH—Tethyan, Higher, and Lesser Himalaya, respectively. Pie charts show proportion of zircons <150 Ma, x/xx is number of <150 Ma grains after data screening/total number of grains. Gray band shows ages characteristic of Transhimalaya of the SLB. Although grains in the range 30–50 Ma occur both in the Transhimalaya (commonly) and Indian plate Himalaya (uncommonly) (e.g., Lang and Huntington, 2014), the fact that none of our Indian-derived samples (SJ1 to SJ7) contain any grains of such age indicates that the 30–50 Ma population is also Transhimalayan-derived at DC.

[1]GSA Data Repository item 2018078, analytical and stress calculation methods and supplementary figures; sample locations (Table DR1); zircon U-Pb ages from source-areas compilation (Table DR2); zircon U-Pb ion probe data and standard (Tables DR3 and DR4); zircon U-Pb laser ablation data and standard (Tables DR5 and DR6); and rutile U-Pb laser ablation data and standard (Table DR7), is available online at http://www.geosociety.org/datarepository/2018/ or on request from editing@geosociety.org.

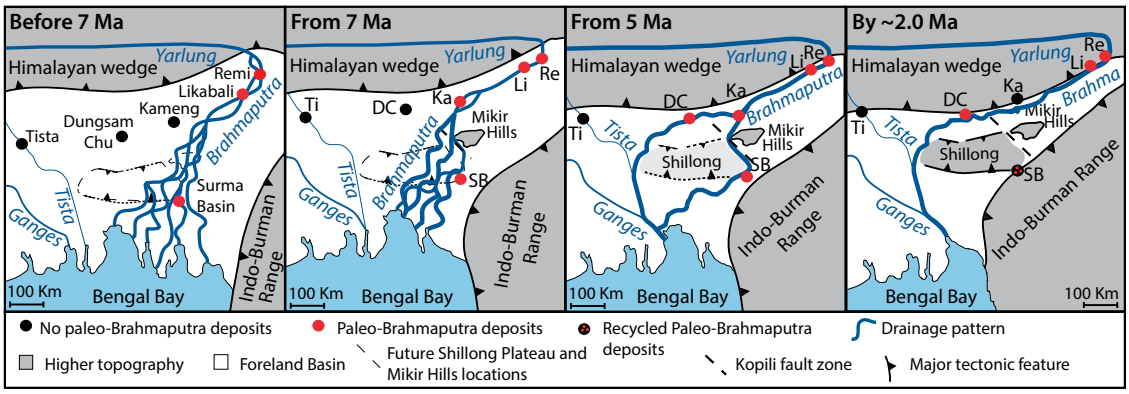

Figure 3. Brahmaputra paleodrainage evolution (modified from Chirouze et al., 2013), constructed using provenance studies from various sedimentary sections: Dungsam Chu (DC, this study); Likabali (Li) (Lang and Huntington, 2014); Remi (Re) (Govin, 2017), Tista (Ti) (Cina et al., 2009) Kameng (Ka) (Chirouze et al., 2013), and Surma Basin (SB) (Bracciali et al., 2015). Position of coastline is ill-constrained and thus the modern position is shown; DC sediments >5 Ma are deltaic (Coutand et al., 2016).

data indicate that the Brahmaputra reached the location of the Kameng section, northeast of the SP (Chirouze et al., 2013; Fig. 3), perhaps due to uplift in the Mikir Hills deflecting the river northward.

Between 4.9 and 5.2 Ma, the Brahmaputra reached DC due to the uplift of the SP deflecting the river northward and westward. However, coeval paleo-Brahmaputra deposits, not recycled from older units (thermochronological ages young up-section), are also found in the Surma Basin to the south of the SP (Bracciali et al., 2015). This can be explained by temporal and spatial variations of displacements on the Oldham and Dauki faults (Biswas et al., 2007), resulting in non-uniform uplift, and repeated switching of the Brahmaputra to courses east and west of the rising plateau.

By ca. 2 Ma, the Brahmaputra course east of the plateau closed due to the combination of westward propagation of the Indo-Burman Ranges and plateau rise (Najman et al., 2016). Since then, the river has flowed exclusively to the north and west of the SP, with Himalayan thrusting deflecting the river progressively south to its current location.

Causes of the Transition from Rock Uplift to Surface Uplift

The time lag between exhumation and surface uplift of the SP has previously been proposed to result from exhumation of basement rocks from beneath the more erodible Cenozoic sediment cover, leading to a decrease in erosion rate (Biswas et al., 2007). However, it was not until after ca. 1.5 Ma that SP basement rocks became the primary contributor to the Surma Basin (Najman et al., 2012; Bracciali et al. 2016). Thus, there appears to be an ~3.5 m.y. lag between our inferred onset of surface uplift (5.2–4.9 Ma) and the time of transition from predominantly cover to basement erosion (after 1.5 Ma), suggesting that the latter is not the dominant factor responsible for the change from exhumation to surface uplift of the SP.

A possible tectonic driver for this change involves an increase in slip rates of the faults bounding the plateau, such that surface denudation could no longer keep pace with rock uplift. Because the SP lies in the foreland being overridden by the Himalaya, the stresses acting on the faults bounding the plateau will have changed through time. Copley et al. (2011) calculated the stress state in the Indian plate due to far-field tectonic forces and bending of the Indian lithosphere beneath the Himalaya, using a model in which the Indian crust is broken by faults (see Data Repository section 2c). Copley et al. (2011) showed that the maximum differential stresses on the faults, and in the upper part of the ductile mantle, increase by a factor of ~1.5 as the Indian lithosphere bends beneath the Himalaya.

Fault-slip rates are thought to be nonlinearly related to the stress state at the base of the seismogenic layer, either through nonlinearity in the rate-state friction equations that describe the loading of faults by aseismic creep on their down-dip extensions (Marone, 1998), or by stress accumulation due to dislocation creep immediately beneath the seismogenic layer (Zoback and Townend, 2001). The nonlinear relationship between applied stress and fault loading rate for both possible mechanisms means that an increase in differential stress near the brittle-ductile transition by a factor of ~1.5 could result in a slip-rate increase by a factor of ≥2 (see Data Repository section 2c). Such an increase in slip rate is a plausible cause for the onset of surface uplift in the SP. The apparent twofold or larger increase in slip rate on the faults bounding the SP in the past ~10 m.y. suggested by Vernant et al., (2014), inferred from comparing modern and Miocene-Pliocene slip rates (Biswas et al., 2007; Clark and Bilham, 2008), provides support for this model.

The time scale for such a change depends on how long it takes the plateau to be transported through the region affected by bending stresses as India underthrusts the Himalaya (the east-west stresses due to loading by the Indo-Burman Ranges affect only the intermediate principal stress, so will not affect the fault-slip rates). The negative gravity anomaly associated with the foreland basin farther west indicates that the region subject to significant bending stresses is ~300 km wide (see Data Repository section 2c). The complex geometry of faults and basins makes this distance difficult to pinpoint in the SP region. However, we assume that the bending stresses occur over a similar distance from the Himalayan front in the SP region as farther west, based upon the similar depth distribution of earthquakes in these two regions (Craig et al., 2012). This logic implies that the SP has been transported ~100–200 km into the region affected by stresses resulting from bending of the Indian lithosphere beneath the Himalaya. At a convergence rate of ~15 mm/yr between the SP and southern Tibet (Vernant et al., 2014), this distance is consistent with the onset timing of exhumation (9–15 Ma) and surface uplift (ca. 5.2–4.9 Ma) in the SP.

Our results imply that the decrease in shortening rate in the Bhutan Himalaya, as a consequence of an increasing proportion of the overall convergence being accommodated by the SP, is likely to have occurred close to the most recent limit of the time range suggested by McQuarrie et al. (2014). The onset of rotation of the Brahmaputra valley relative to the Indian subcontinent described by Vernant et al. (2014) must have begun earlier, in order to allow the shortening that led to exhumation in the SP at 9–15 Ma, but to have accelerated at ca. 5 Ma. Our results imply that the presence and rate of this rotation are controlled not only by far-field tectonic stresses and pre-existing lithospheric structure (such as the transition from continental to thinned continental or oceanic crust, which coincides with the location of the SP), but also by bending of the foreland lithosphere beneath the Himalaya.

CONCLUSIONS

We date the initiation of topographic growth of the Shillong Plateau to between 4.9 and 5.2 Ma. Rock uplift in the plateau was balanced by surface erosion between 9 and 15 Ma and 5.2–4.9 Ma, such that no topography was created. We link plateau uplift to accelerated displacement along the Dauki fault, caused by bending stresses resulting from northward underthrusting of the Indian plate beneath Tibet. By incorporating the full

range of available observations, we have pinpointed the transition from exhumation balanced by erosion to topographic growth, and suggest this previously unrecognized mechanism for the transition.

ACKNOWLEDGMENTS

This work was supported by the European Union Executive Agency For Research FP7 MC ITN "iTECC" (Investigating Tectonics Erosion Climate Couplings) grant 316966 and Natural Environment Research Council Isotope Geosciences Laboratory FSC grant IP-1500–1114. We thank six reviewers and editor J. Schmitt for comments. Gwladys Govin died while this paper was in review; final edits were carried out by the co-authors.

REFERENCES CITED

Biswas, S., Coutand, I., Grujic, D., Hager, C., Stockli, D., and Grasemann, B., 2007, Exhumation and uplift of the Shillong Plateau and its influence on the eastern Himalayas: New constraints from apatite and zircon (U-Th-[Sm])/He and apatite fission track analysis: Tectonics, v. 26, TC6013, https://doi.org/10.1029/2007TC002125.

Bracciali, L., Najman, Y., Parrish, R.R., Akhter, S.H., and Millar, I., 2015, The Brahmaputra tale of tectonics and erosion: Early Miocene river capture in the Eastern Himalaya: Earth and Planetary Science Letters, v. 415, p. 25–37, https://doi.org/10.1016/j.epsl.2015.01.022.

Bracciali, L., Parrish, R.R., Najman, Y., Smye, A., Carter, A., and Wijbrans, J.R., 2016, Plio-Pleistocene exhumation of the eastern Himalayan syntaxis and its domal 'pop-up': Earth-Science Reviews, v. 160, p. 350–385, https://doi.org/10.1016/j.earscirev.2016.07.010.

Chirouze, F., Huyghe, P., van der Beek, P., Chauvel, C., Chakraborty, T., Dupont-Nivet, G., and Bernet, M., 2013, Tectonics, exhumation, and drainage evolution of the eastern Himalaya since 13 Ma from detrital geochemistry and thermochronology, Kameng River Section, Arunachal Pradesh: Geological Society of America Bulletin, v. 125, p. 523–538, https://doi.org/10.1130/B30697.1.

Cina, S.E., Yin, A., Grove, M., Dubey, C.S., Shukla, D.P., Lovera, O.M., Kelty, T.K., Gehrels, G.E., and Foster, D.A., 2009, Gangdese arc detritus within the eastern Himalayan Neogene foreland basin: Implications for the Neogene evolution of the Yalu-Brahmaputra River system: Earth and Planetary Science Letters, v. 285, p. 150–162, https://doi.org/10.1016/j.epsl.2009.06.005.

Clark, M.K., and Bilham, R., 2008, Miocene rise of the Shillong Plateau and the beginning of the end for the Eastern Himalaya: Earth and Planetary Science Letters, v. 269, p. 337–351, https://doi.org/10.1016/j.epsl.2008.01.045.

Copley, A., Avouac, J.P., Hollingsworth, J., and Leprince, S., 2011, The 2001 Mw 7.6 Bhuj earthquake, low fault friction, and the crustal support of plate driving forces in India: Journal of Geophysical Research. Solid Earth, v. 116, B08405, 10.1029/2010JB008137.

Coutand, I., Barrier, L., Govin, G., Grujic, D., Hoorn, C., Dupont-Nivet, G., and Najman, Y., 2016, Late Miocene-Pleistocene evolution of India-Eurasia convergence partitioning between the Bhutan Himalaya and the Shillong Plateau: New evidences from foreland basin deposits along the Dungsam Chu section, eastern Bhutan: Tectonics, v. 35, p. 2963–2994, https://doi.org/10.1002/2016TC004258.

Coutand, I., Whipp, D.M., Grujic, D., Bernet, M., Fellin, M.G., Bookhagen, B., Landry, K.R., Ghalley, S.K., and Duncan, C., 2014, Geometry and kinematics of the Main Himalayan Thrust and Neogene crustal exhumation in the Bhutanese Himalaya derived from inversion of multithermochronologic data: Journal of Geophysical Research: Solid Earth, v. 119, p. 1446–1481, https://doi.org/10.1002/2013JB010891.

Craig, T.J., Copley, A., and Jackson, J., 2012, Thermal and tectonic consequences of India underthrusting Tibet: Earth and Planetary Science Letters, v. 353–354, p. 231–239, https://doi.org/10.1016/j.epsl.2012.07.010.

England, P.C., and Bilham, R., 2015, The Shillong Plateau and the great 1897 Assam Earthquake: Tectonics, v. 34, p. 1792–1812, https://doi.org/10.1002/2015TC003902.

Gehrels, G., Kapp, P., DeCelles, P., Pullen, A., Blakey, R., Weislogel, A., Ding, L., Guynn, J., Martin, A., and McQuarrie, N., 2011, Detrital zircon geochronology of pre-Tertiary strata in the Tibetan-Himalayan orogen: Tectonics, v. 30, TC5016, https://doi.org/10.1029/2011TC002868.

Govin, G., 2017, Tectonic-Erosion Interactions: Insights from the palaeo-drainage of the Brahmaputra River [Ph.D. thesis]: Lancaster, UK, Lancaster University, 331 p., https://doi.org/10.17635/lancaster/thesis/116.

Grujic, D., Coutand, I., Bookhagen, B., Bonnet, S., Blythe, A., and Duncan, C., 2006, Climatic forcing of erosion, landscape and tectonics in the Bhutan Himalayas: Geology, v. 34, p. 801–804, https://doi.org/10.1130/G22648.1.

Hu, X., Sinclair, H.D., Wang, J., Jiang, H., and Wu, F., 2012, Late Cretaceous-Palaeogene stratigraphic and basin evolution in the Zhepure Mountain of southern Tibet: Implications for the timing of India-Asia initial collision: Basin Research, v. 24, p. 520–543, https://doi.org/10.1111/j.1365-2117.2012.00543.x.

Johnson, S.Y., and Alam, A.M.N., 1991, Sedimentation and tectonics of the Sylhet trough, Bangladesh: Geological Society of America Bulletin, v. 103, p. 1513–1527, https://doi.org/10.1130/0016-7606(1991)103<1513:SATOTS>2.3.CO;2.

Jordan, T.E., and Allmendinger, R.W., 1986, The Sierras Pampeanas of Argentina—A modern analogue of Rocky-mountain foreland deformation: American Journal of Science, v. 286, p. 737–764, https://doi.org/10.2475/ajs.286.10.737.

Kober, M., Seib, N., Kley, J., and Voigt, T., 2013, Thick-skinned thrusting in the northern Tien Shan foreland, Kazakhstan: Structural inheritance and polyphase deformation: Geological Society of London Special Publications, v. 377, p. 19–42, https://doi.org/10.1144/SP377.7.

Lang, K.A., and Huntington, K.W., 2014, Antecedence of the Yarlung-Siang-Brahmaputra River, eastern Himalaya: Earth and Planetary Science Letters, v. 397, p. 145–158, https://doi.org/10.1016/j.epsl.2014.04.026.

Lang, K.A., Huntington, K.W., Burmester, R., and Housen, B., 2016, Rapid exhumation of the eastern Himalayan syntaxis since the Late Miocene: Geological Society of America Bulletin, v. 128, p. 1403–1422, https://doi.org/10.1130/B31419.1.

Long, S., McQuarrie, N., Tobgay, T., Grujic, D., and Hollister, L.S., 2011, Geological map of Bhutan: Journal of Maps, v. 7, p. 184–192, https://doi.org/10.4113/jom.2011.1159.

Marone, C., 1998, Laboratory-derived friction laws and their application to seismic faulting: Annual Review of Earth and Planetary Sciences, v. 26, p. 643–696, https://doi.org/10.1146/annurev.earth.26.1.643.

McQuarrie, N., Tobgay, T., Long, S., Reiners, P., and Cosca, M., 2014, Variable exhumation rates and variable displacement rates: Documenting recent slowing of Himalayan shortening in western Bhutan: Earth and Planetary Science Letters, v. 386, p. 161–174, https://doi.org/10.1016/j.epsl.2013.10.045.

Mitra, S., and Mitra, S., 2001, Tectonic setting of the Precambrian of the northeastern India (Meghalaya Plateau) and age of the Shillong Group of rocks: Geological Survey of India Special Publication, v. 64, p. 653–658.

Mitra, S., Priestley, K., Bhattacharyya, A.K., and Gaur, V., 2005, Crustal structure and earthquake focal depths beneath northeastern India and southern Tibet: Geophysical Journal International, v. 160, p. 227–248, https://doi.org/10.1111/j.1365-246X.2004.02470.x.

Najman, Y., Allen, R., Willett, E., Carter, A., Barfod, D., Garzanti, E., Wijbrans, J., Bickle, M., Vezzoli, G., and Ando, S., 2012, The record of Himalayan erosion preserved in the sedimentary rocks of the Hatia Trough of the Bengal Basin and the Chittagong Hill Tracts, Bangladesh: Basin Research, v. 24, p. 499–519, https://doi.org/10.1111/j.1365-2117.2011.00540.x.

Najman, Y., Bracciali, L., Parrish, R.R., Chisty, E., and Copley, A., 2016, Evolving strain partitioning in the Eastern Himalaya: The growth of the Shillong Plateau: Earth and Planetary Science Letters, v. 433, p. 1–9, https://doi.org/10.1016/j.epsl.2015.10.017.

Rosenkranz, R., Schildgen, T., Wittmann, H., and Spiegel, C., 2018, Coupling erosion and topographic development in the rainiest place on Earth: Reconstructing the Shillong Plateau uplift history with in-situ cosmogenic ^{10}Be: Earth and Planetary Science Letters, v. 483, p. 39–51, https://doi.org/10.1016/j.epsl.2017.11.047.

Seeber, L., and Armbruster, J.G., 1981, Great detachment earthquakes along the Himalayan Arc and long-term forecasting, *in* Simpson, D.W., and Richards, P.G., eds., Earthquake Prediction: An International Review: American Geophysical Union, Maurice Ewing Series, v. 4, p. 259–277, https://doi.org/10.1029/ME004p0259.

Singh, A., Bhushan, K., Singh, C., Steckler, M.S., Akhter, S.H., Seeber, L., Kim, W.Y., Tiwari, A.K., and Biswas, R., 2016, Crustal structure and tectonics of Bangladesh: New constraints from inversion of receiver functions: Tectonophysics, v. 680, p. 99–112, https://doi.org/10.1016/j.tecto.2016.04.046.

Uddin, A., and Lundberg, N., 1999, A paleo-Brahmaputra? Subsurface lithofacies analysis of Miocene deltaic sediments in the Himalayan–Bengal system, Bangladesh: Sedimentary Geology, v. 123, p. 239–254, https://doi.org/10.1016/S0037-0738(98)00134-1.

Vermeesch, P., 2012, On the visualisation of detrital age distributions: Chemical Geology, v. 312–313, p. 190–194, https://doi.org/10.1016/j.chemgeo.2012.04.021.

Vernant, P., Bilham, R., Szeliga, W., Drupka, D., Kalita, S., Bhattacharyya, A., Gaur, V., Pelgay, P., Cattin, R., and Berthet, T., 2014, Clockwise rotation of the Brahmaputra Valley relative to India: Tectonic convergence in the eastern Himalaya, Naga Hills, and Shillong Plateau: Journal of Geophysical Research: Solid Earth, v. 119, p. 6558–6571, https://doi.org/10.1002/2014JB011196.

Zoback, M.D., and Townend, J., 2001, Implications of hydrostatic pore pressures and high crustal strength for the deformation of intraplate lithosphere: Tectonophysics, v. 336, p. 19–30, https://doi.org/10.1016/S0040-1951(01)00091-9.

Manuscript received 3 November 2017
Revised manuscript received 23 December 2017
Manuscript accepted 27 December 2017

Printed in USA